

# Design and characterization of a soft magneto-rheological miniature shock absorber for a controllable variable stiffness sole

DANIEL GRIVON<sup>1</sup>, YOAN CIVET<sup>1</sup>, ZOLTAN PATAKY<sup>2</sup>, YVES PERRIARD<sup>1</sup>

<sup>1</sup> *École Polytechnique Fédérale de Lausanne  
Institut de Microtechnique (IMT), Laboratoire d'Actionneurs Intégrés (LAI)  
Rue de la Maladière, 71 B, 2002 Neuchâtel, Switzerland  
e-mail: daniel.grivon@epfl.ch*

<sup>2</sup> *Service of Therapeutic Education for Chronic Diseases, WHO Collaborating Center  
Geneva University Hospital and University of Geneva  
Rue de Gabrielle-Perret-Gentil 4, 1205, Geneva, Switzerland*

(Received: 02.09.2015, revised: 20.09.2015)

**Abstract:** The proposed paper discusses the design and characterization of a soft miniature Magneto-Rheological (MR) shock absorber. In particular, the final application considered for the insertion of the designed devices is a controllable variable stiffness sole for patients with foot neuropathy. Such application imposes particularly challenging constraints in terms of miniaturization (cross-sectional area  $\leq 1.5 \text{ cm}^2$ , height  $\leq 25 \text{ mm}$ ) and high sustainable loads (normal loads up to 60 N and shear stresses at the foot/device interface up to 80 kPa) while ensuring moderate to low level of power consumption. Initial design considerations are done to introduce and justify the chosen novel configuration of soft shock absorber embedding a MR valve as the core control element. Successively, the dimensioning of two different MR valves typologies is discussed. In particular, for each configuration two design scenarios are evaluated and consequently two sets of valves satisfying different specifications are manufactured. The obtained prototypes result in miniature modules (external diam.  $\leq 15 \text{ mm}$ , overall height  $\leq 30 \text{ mm}$ ) with low power consumption (from a minimum of 63 mW to a max. of 110 mW) and able to sustain a load up to 65 N. Finally, experimental sessions are performed to test the behaviour of the realized shock absorbers and results are presented.

**Key words:** magneto-rheological fluid, miniaturization, soft shock absorber, design and characterization

## 1. Introduction

Magneto-Rheological (MR) fluids are a particular kind of smart fluids consisting of micrometer range magnetic particles (typically 1 to 10  $\mu\text{m}$ ) suspended in a non-magnetic liquid carrier, usually oil or water [1]. The main properties of MR fluids is related to the capability to change their physical features through the influence of a magnetic field. If excited by an external

magnetic field, the filling particles behave like magnetic dipoles interacting with each other to form chain-like structures aligned parallel to the magnetic field (Fig. 1) [2].

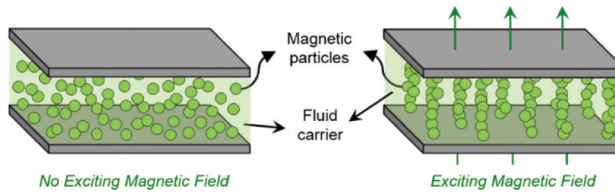


Fig. 1. Magneto-rheological phenomenon

The strength of the attractive force between adjacent particles is mainly related to the magnitude and distribution of the exciting magnetic field  $H$ . This latter determines the raise of a magnetic field dependent yield stress  $\tau_y(H)$  required to deform the chains-like structures and obtain a flow variation. MRFs are thus defined as *non-newtonian* fluids with controllable yield stress and they are usually described using the Bingham model (Fig. 2) [3]

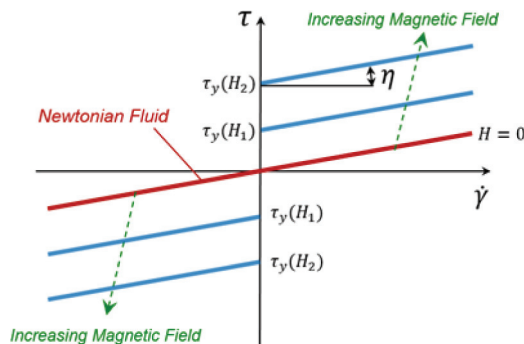


Fig. 2. Bingham materials – shear stress Vs shear strain

$$\begin{cases} \tau = \tau_y(H) + \eta\dot{\gamma}, & |\tau| > \tau_y \\ \dot{\gamma} = 0, & |\tau| \leq \tau_y, \end{cases} \quad (1)$$

where  $\tau$  is the overall fluid yield stress,  $\eta$  is the fluid viscosity and  $\dot{\gamma}$  is the shear rate.

This phenomenon, which locally changes the internal yield stress of the fluid, i.e. its viscosity, has been used extensively in the design of power dissipating devices such as valves, clutches, brakes and dampers [4].

Magneto-Rheological dampers have been widely employed in a variety of different applications and domains, ranging from automotive to civil or structural engineering, to realize controllable shock absorbers [5].

The common configuration of a MR damper consists of a piston-like design in which the fluid flow between the first and second chamber is regulated using a MR valve connected with the piston rod and able to displace along the damper symmetry axis (Fig. 3).

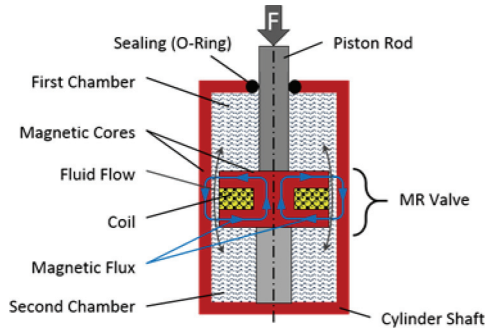


Fig. 3. Basic MR damper configuration

The fluid flow between the first and the second chamber due to the valve vertical displacement is orthogonally crossed by the magnetic flux produced by the coil embedded in the MR valve. This latter induces a change in the viscosity of the MR fluid and a consequent increase in its resistance to flow. Consequently, a pressure drop rises between the two chambers and the damper sustainable force increases. The total amount of force sustainable by the damper can be thus expressed as the sum of the viscosity dependent force  $F_\eta$  and the magnetic field dependent force  $F_\tau(H)$  [6]

$$F = F_\eta + F_\tau(H) = \frac{\eta SA}{g} + \tau_y(H)A, \quad (2)$$

where  $S$  is the piston rod velocity,  $A$  is the active surface and  $g$  is the channel gap.

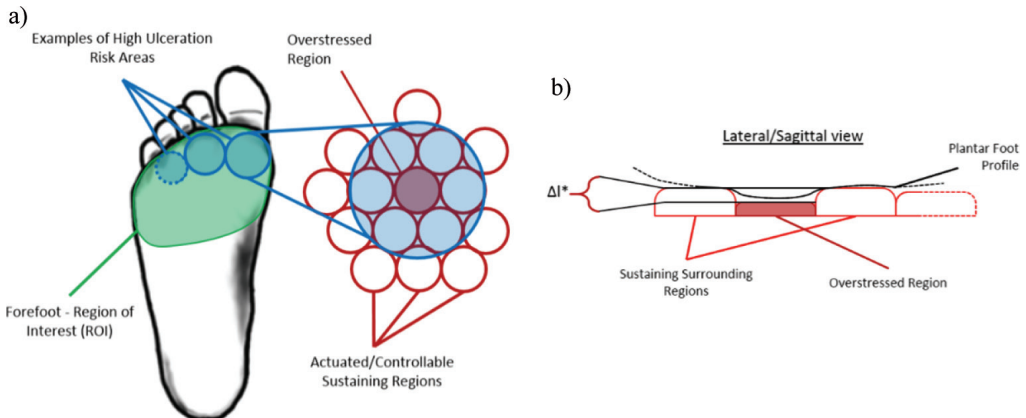


Fig. 4. a) Foot plantar, Regions of Interest and modules placement. b) – Proposed offloading strategy

Although the design methodology, the features as well as the achievable results of such configuration are well-known, important feasibility and reliability issues may arise in the case of high miniaturization constraints and high applied loads. In particular, the final application embedding the MR miniature shock absorbers consists in a variable stiffness sole for people with

foot neuropathy and undergoing plantar ulcerations. In this scenario, the designed device will be used to locally control the hardness of the sole at the foot contact and redistribute pressure to avoid the rise of undesired overstressed regions. Figure 4a illustrates the foreseen module placement under the foot region of interest while Figure 4b depicts the approach intended to off-load the foot plantar. If an overstressed region is detected, the corresponding shock absorber is controlled to be as soft as possible while the surrounding modules are maintained stiff. This way a depression is created in the insole allowing to locally relieve the foot plantar pressure (Fig. 4).

## 2. Soft MR shock absorbers design

As introduced, the miniaturization process is crucial for the particular application considered and it may be critical if abruptly applied to the common MR damper configurations. Severe guiding and sealing problems are expected among parts in relative motion if it is considered that the load transmitted by the foot to the damper is not purely axial, but it includes a remarkable radial component. In fact, plantar shear stresses during the foot ground contact are not negligible and have been estimated to range from 30 up to more than 80 kPa [7, 8]. In this case, dedicated structures are required to adequately address these issues, but they can result in a not admitted increase of the bulkiness of the overall device. These issues together with the need to provide a smooth interface with the loading body (foot plantar tissues), lead to the design of a novel soft shock absorber configuration in which no parts in relative motion to each other are present [9]. The vertical displacement under an applied load is controlled regulating the outflow of a MR fluid from an external deformable cushion. The total shock absorber stroke imposed by the final application is 3 mm. Once load is removed, the damper initial state is restored thanks to an elastic reflow membrane which brings back up the MR fluid into the deformable cushion (Fig. 5).

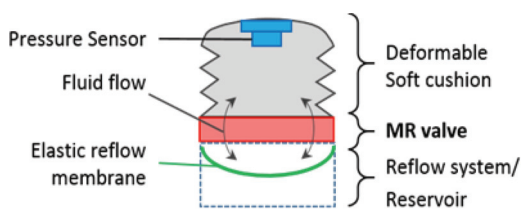


Fig. 5. Schematic representation of the proposed MR soft shock absorber

Consequently, the MR valve represents the key control element as well as the component which will mostly affect the damper behaviour and its performances. The common design of MR valves usually considers valves with an annular channel, but recent studies have investigated configurations with radial flow of MR fluid and both radial and annular flow at the same time. Regarding this last point, a preliminary study concerning the dimensioning and the comparison of these three different valve configurations has already been discussed in [10] and it will be used as a design tool in the presented work.

In particular, considering the results of the performed analysis and in order to compare the performances achievable with different valve typologies, both a more common annular configuration and a new radial MR valve have been dimensioned. For an annular MR valve (Fig. 3a), the total sustainable pressure drop is [11]

$$\Delta P = \Delta P_\tau + \Delta P_\eta = \frac{c\tau_y(H)h}{g} + \frac{6\eta Qh}{g^3\pi r_g}, \quad (3)$$

while for a radial configuration (Fig. 3b) we have [11]

$$\Delta P = \Delta P_\tau + \Delta P_\eta = \frac{c\tau_y(H)(r_e - r_i)}{g} + \frac{6\eta Q}{g^3\pi} \cdot \ln\left(\frac{r_e}{r_i}\right), \quad (4)$$

where  $\Delta P_\tau$  is the magnetic field dependent pressure drop,  $\Delta P_\eta$  is the viscosity dependent pressure drop,  $Q$  is the valve flow rate without any exciting magnetic field,  $c$  is a fluid coefficient ranging from a minimum value of 2 ( $\Delta P_\tau/\Delta P_\eta \approx 1$ ) up to a maximum value of 3 ( $\Delta P_\tau/\Delta P_\eta \geq 100$ ), while the remaining geometrical parameters are displayed in Fig. 6a and 6b. It is straightforward that the maximum sustainable pressure  $\Delta P$  and the fluid flow rate  $Q$  can be related to the sustainable force (i.e. the load imposed by the foot during daily walking activities for the particular application considered) and the velocity of the dampers described in (2) using simple geometrical considerations.

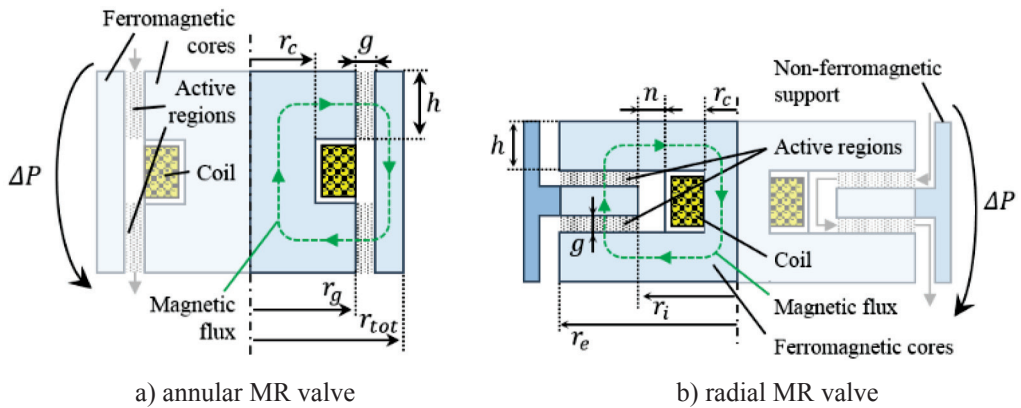


Fig. 6. Schematic cross-section of the MR valve configurations evaluated for the proposed damper

In [10] the authors define the relevant analytical formulae to relate the valves geometrical parameters to the magnetic and electric quantities required to satisfy some imposed design for each of the valve configurations discussed. Following the approach used in this preliminary analysis, a complete system of equation can be built for both the annular (5) and radial valves (6) in order to obtain all the unknown geometrical parameters given the maximum sustainable pressure  $\Delta P_{\tau \max}$ , the dynamic ratio  $D = \Delta P_{\tau \max} / \Delta P_\eta$ , the maximum allowed current density  $J$  and the flow rate  $Q$  without any exciting magnetic field  $H$

$$\left\{ \begin{array}{l} \Delta P_{\tau_{\max}} = \frac{2ch\alpha}{\mu_0\mu_{MR}g} B_{MR} \\ D = \frac{c\alpha\pi g^2 r_g h}{3\eta\mu_0\mu_{MR}Q \left( 2h + \sqrt{\frac{2g}{\mu_0\mu_{MR}J\chi}} \right)} B_{MR} \\ \left( r_g - \sqrt{2r_g h\gamma} \right)^2 = \frac{2g}{\mu_0\mu_{MR}J\chi} B_{MR} \end{array} \right. \quad (5)$$

$$\left\{ \begin{array}{l} \Delta P_{\tau_{\max}} = \frac{2c(r_e - r_i)\alpha}{\mu_0\mu_{MR}g} B_{MR} \\ D = \frac{c\alpha\pi g^2 (r_e - r_i)}{3\eta\mu_0\mu_{MR}Q \cdot \ln(r_e / r_i)} B_{MR} \\ \left( r_i - n - \gamma \cdot \sqrt{r_e^2 - r_i^2} \right)^2 = \frac{2g}{\mu_0\mu_{MR}J\chi} B_{MR} \\ \xi \cdot \frac{\Delta P_{\tau_{\max}}}{D} = \frac{6\eta Q (r_i - n - r_e - 2g)}{\pi (r_i - n)n^3}, \end{array} \right. \quad (6)$$

where  $\alpha$  is a constant and  $\mu_{MR}$  the relative permeability of the considered MR fluid,  $\gamma = B_{MR}/B_{iron}$  is the maximum ratio between the induction through the MR fluid  $B_{MR}$  and the magnetic saturation of the iron cores  $B_{iron}$ ,  $\chi$ , is coil filling factor and  $\xi$  is a coefficient defining the relevance of the viscosity pressure drop across the annular channel located at the interface with the coil with respect to the overall viscosity pressure drop  $\Delta P_{\eta}$  estimated for the valve.

Once the parameters related to the employed materials are fixed, the only remaining coefficients to be imposed are the input parameters allowing the overall dimensioning of the desired valve (as schematically described in Fig. 7 for the case of an annular configuration).

For each valve design, two different requirement scenarios have been fixed as presented in the following table.

Table 1. MR valve requirements for the two design scenarios considered

Scenario	$\Delta P$ [kPa]	$Q$ [cm <sup>3</sup> /s]	$J$ [A/mm <sup>2</sup> ]	$B_{MR}$ [T]
#1	1000	1	6	0.7
#2	1500			

In particular, the maximum sustainable pressure  $\Delta P$  is fixed considering a safety margin with respect to the maximum foot plantar pressure expected which can reach up to 600 kPa. The flow rate  $Q$  is defined in order to guarantee a sufficiently quick emptying of the soft deformable cushion and, consequently, a rapid flattening of the damper. The low value of current density  $J$  is used to avoid high temperature in the coil and an overheating of the MR valve if the device

is maintained on for long intervals, while  $B_{MR}$  represents the maximum magnetic induction through the fluid before saturation.

The fluid used in the damper is the MRF132DG provided by Lord Corporation [13] with viscosity  $\eta = 0.092 \text{ Pa}\cdot\text{s}^{-1}$  and  $\alpha = 0.22 \text{ Pa}\cdot\text{m}\cdot\text{A}^{-1}$ , while for what concerns the coil, the wire used has a nominal diameter of 0.25 mm and a filling factor  $\chi = 0.7$  has been considered. The design of the magnetic circuit has been done to avoid saturation for values of current densities lower than the imposed  $J$  and fixing a maximum induction in the iron cores  $B_{\text{iron}} = 1.32 \text{ T}$ . In particular, these latter have been manufactured using ARMCO soft magnetic steel which guarantees a higher level of saturation induction (up to 2.15 T) [14]. This design choice is used as a safe factor to eventually increase the supply current during the test phase without occurring in the saturation of the ferromagnetic valve cores.

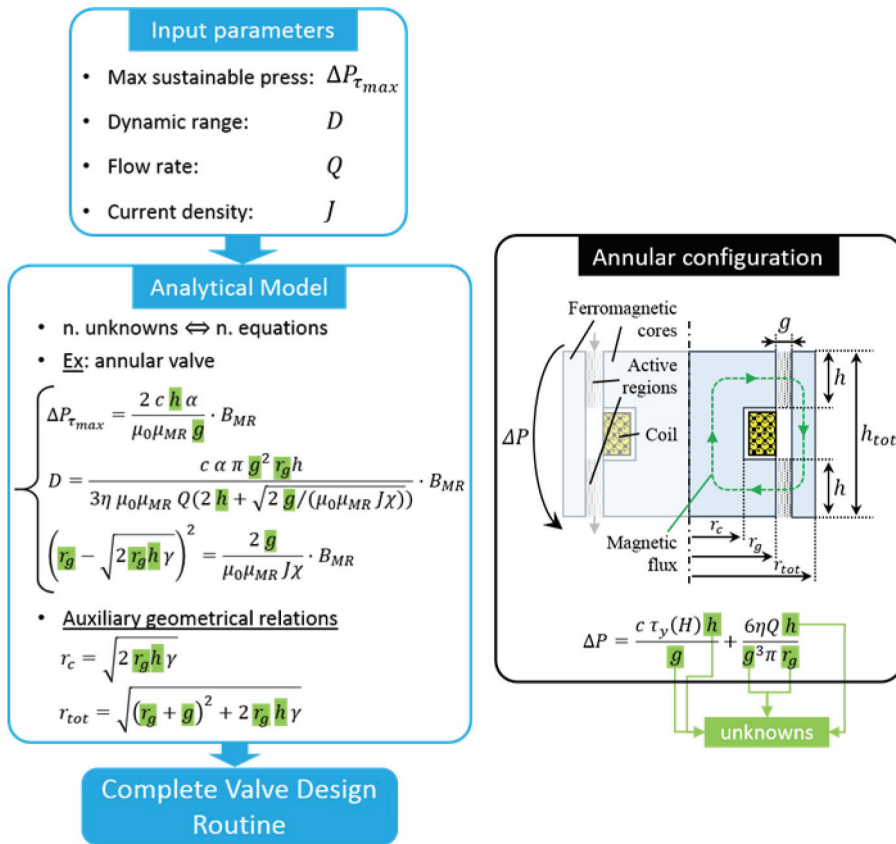


Fig. 7. Schematic flow chart representation of the design methodology used to dimension the MR valves (in the represented case an annular design is taken in consideration)

Table 2 reports the most significant parameters defining the different MR valves designed. Concerning the number of turns and the resistance of the manufactured coils, both the exact values issued from the preliminary dimensioning (in brackets) and the real values are reported.

Finally, Figure 8 depicts two of the four manufactured shock absorbers embedding respectively a radial and an annular MR valve realized accordingly to dimensions listed in Table 2 for the design scenario #1.

Table 2. MR valves parameters for the two design scenarios (geometrical dimensions are expressed in [mm]). The coil number of turns and the measured resistance are also reported

Scenario #1						
	$h$	$r_g$		$g$	$N$ of Turns	$R_{coil}$ [ $\Omega$ ]
Annular	1	4.4		0.1	67 (68)	0.68 (0.53)
		$r_e$	$r_i$			
Radial	1	4.6	3.9	0.08	31 (41)	0.25 (20)
Scenario #2						
		$r_g$		$g$	N. of Turns	$R_{coil}$ [ $\Omega$ ]
Annular	1.3	4.7		0.1	71 (70)	0.70 (0.56)
		$r_e$	$r_i$			
Radial	1.1	5.2	4.2	0.08	34 (39)	0.28 (0.21)

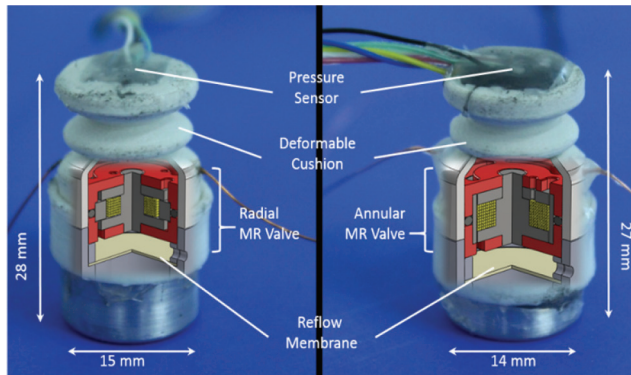


Fig. 8. Two shock absorbers including a radial a) and an annular b) MR valve. The cross-sectional view allows to depict the actual implementation of the two MR valve designs

### 3. Experimental session and results

In order to characterize both the performances of the different miniature soft MR shock absorbers manufactured, a simple, but effective experimental bench test has been realized (Fig. 9).

The load is applied using a compressed air piston able to exercise a maximum load of 100 N at a maximum frequency of 10 Hz. The pressure of the MR fluid internal to the deformable cushion is measured using a pressure sensor (embedded within the cushion itself) which allows a maximum sampling frequency of 1 kHz and a maximum resolution of 12 bits. The displace-

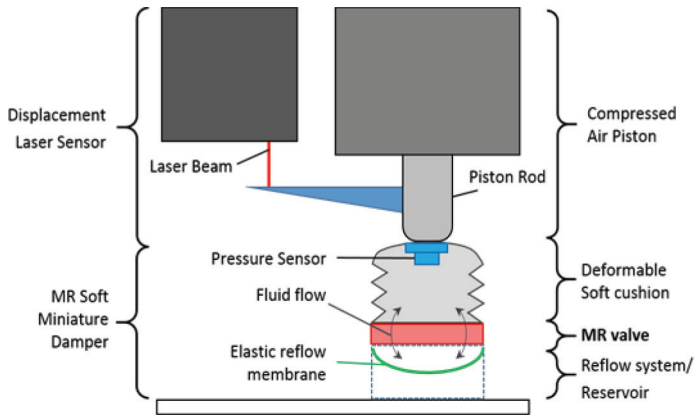


Fig. 9. A schematic representation of the experimental setup used for the characterization of the soft miniature MR dampers

ment of the loading piston rod, which corresponds to the vertical deformation of the soft cushion, is measured using an optical laser sensor.

The performed tests consist in applying a constant load of 65 N to the shock absorber while this latter is supplied with different current densities. In particular, the value of  $J$  imposed for each device and thus, valve configurations, ranges from a minimum of 0 to a maximum of  $8.1 \text{ A}\cdot\text{mm}^{-2}$ , this latter value exceeding the imposed maximum current density defined in the aforementioned design scenario. This choice is used to compensate the fact that, as previously introduced, the number of turns resulting from the MR valve dimensioning is not perfectly matched for all the configurations. Furthermore, such a leeway in the imposable current supply before occurring in saturation of the valve magnetic cores can be used as a mean to verify the correctness of the magnetic modelling used in the MR valve design. If increasing the supply current the device performances in terms of sustainable pressure remain unchanged the saturation value of  $B_{MR}$  is reached, meaning that the design features are effectively matched.

After an initial interval of 2 s the piston is activated and the modules are turned on for a total time of 3 s and then are switched off while the load is still maintained.

Finally, after 7 s the load is removed releasing the compressed air in the piston rod. The deformation characteristics for the different measurement sessions are depicted in Figure 10.

All the characteristics depict an initial large vertical deformation of the cushion even when the module is in the locked state (1 to 1.5 mm between 2 and 3 s). This phenomenon can be explained considering that the cushion is made of soft material and that the undergoing deformations are not only vertical, but they can be also radial. Thus, if the volume of filling fluid in the cushion is maintained constant a radial enlargement will be compensated with a further vertical deformation.

Furthermore, some air could be remained trapped before the sealing procedure and its compression can enhance this phenomenon. Nevertheless, as previously introduced, the final application in which the tested shock absorbers will be inserted is a therapeutic shoe for plantar pressure redistribution. As a consequence, such behaviour does not represent a drawback, on the contrary it fulfils the system requirements providing a further intrinsically soft interface for the foot contact.

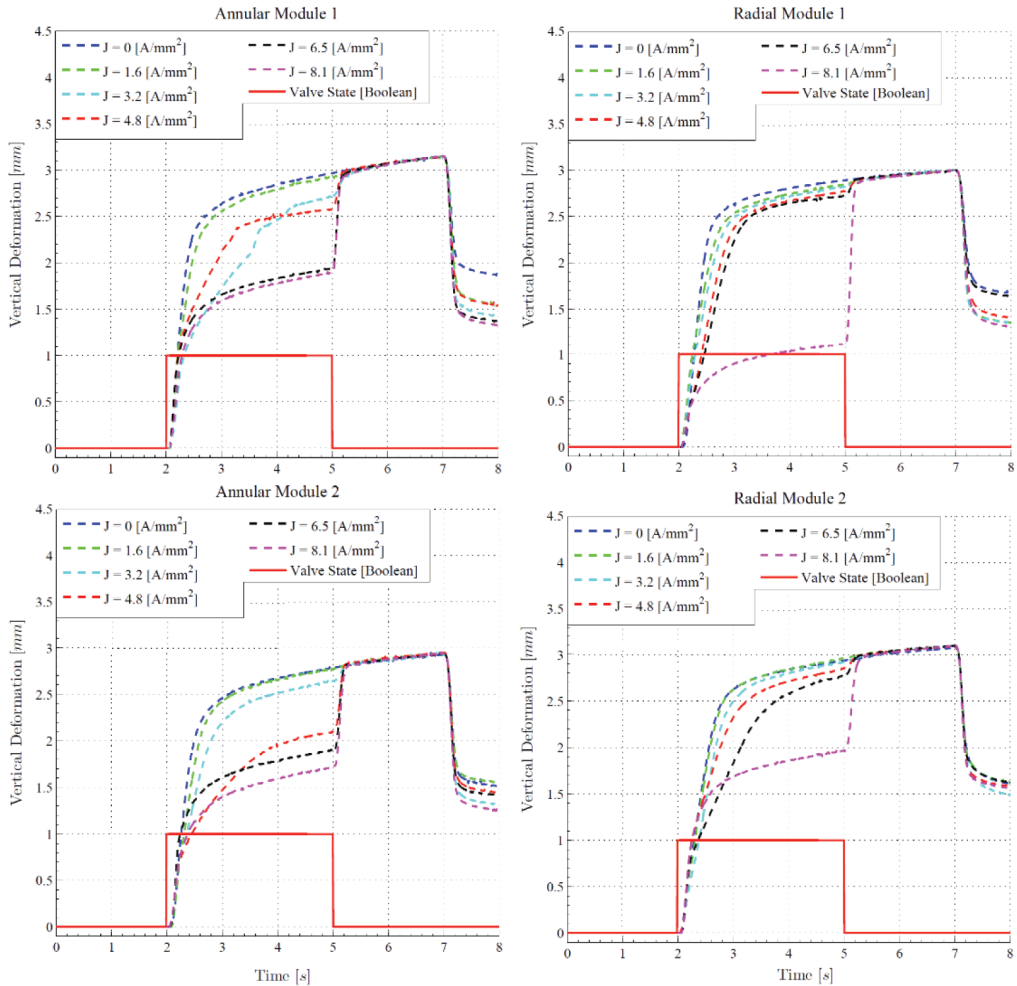


Fig. 10. Results of the measurements performed for the different shock absorbers under test

For increasing values of current density the slope of the initial part of the deformation characteristic, which is related to the flow rate through the MR valve, reduces. Thus, the stiffness of the shock absorbers can be actually controlled regulating the supply current. Considering this last point, if annular and radial modules are compared, it appears that radial valves offer a better controllability, providing a higher flow rate change (i.e. deformation change) for the same supply current change.

All the tested modules succeeded in sustaining the applied load of 6.5 N achieving a blocked state for which the vertical deformation is maintained almost constant (a residual outflow bias still persists, but with respect to the overall actuators stroke and the considered time scale it can be considered negligible). In particular, this result validates the possibility to realize the intended offloading strategy. Nevertheless, while absorbers embedding an annular MR valve satisfy this condition for current densities within the limit fixed by the design scenario of Table 1

( $J = 6.5 \text{ A}\cdot\text{mm}^{-2}$ ) and even an increase of the coil current density up to  $J = 8.1 \text{ A}\cdot\text{mm}^{-2}$  does not change the modules response, radial valve based modules require a higher current supply to achieve this state. This phenomenon can be explained considering that the coil number of turns is not matched for radial modules and, consequently, a current density proportionally higher is required to obtain the same magnetic potential defined during the dimensioning phase and achieve the imposed value of magnetic induction over the MR fluid surface. A further explanation of this phenomenon can be found considering that the analytical approximations introduced to describe the magnetic circuit of the radial MR valve are quite rough. In fact, as described in [10], the unconsidered fringing phenomena and leakage flux result in an approximate magnetic modelling which can partially justify the required boost of  $J$  to achieve the desired magnetic induction  $B_{MR}$ .

The last part of the characteristics shows the tendency of the shock absorbers to restore the initial undeformed state as soon as compressed air is released from the loading piston, thanks both to the intrinsic cushion stiffness and to the reflow membrane, highlighting the validity of the design solutions employed. Only because of residual load due to piston internal friction the initial cushion shape is not restored.

As a final benchmark, the following table reports the different shock absorbers power consumption evaluated as Joule losses in the case of maximum current density required to achieve the maximum measured module stiffness.

Table 3. Power consumption of the different evaluated shock absorbers

	<b>Annular 1</b>	<b>Annular 1</b>	<b>Radial 1</b>	<b>Radial 2</b>
Joule Losses [mW]	109	112	63	70

The main results of Table 3 is related to the low power consumption of the shock absorbers embedding radial MR valves, which is 42-44% lower than modules based on MR annular valve configuration, which underlined the effectiveness and reliability of this novel design regardless to the higher than desired values of current density.

## 4. Conclusion

The proposed paper discusses the design and the characterization of a miniature shock absorber to be inserted in a therapeutic shoe for plantar pressure redistribution.

Initial considerations regarding the final application are made in order to introduce the challenging design scenario, which mainly includes high sustainable load (normal loads up to 60 N and shear stresses at the foot/device interface up to 80 kPa) and strict constraints in terms of miniaturization (cross-sectional area  $\leq 15 \text{ cm}^2$  overall height  $\leq 25 \text{ mm}$ ) and power consumption. Two requirements scenarios are defined and for each one two shock absorbers respectively based on MR valves with annular or radial configurations are designed.

Results obtained from the performed test sessions underline the effectiveness and reliability of the proposed designs, both for what concerns the solutions employed in the conception of the shock absorbers as well as in the dimensioning of the MR valves inserted in the modules which

fulfil all the imposed system requirements. In particular, shock absorbers based on MR radial valves offer better performances in terms of lower power consumption (with a reduction of about 42-44%) and higher module stiffness controllability. Nevertheless, it emerges that radial MR valves require higher current densities to achieve the desired values of magnetic induction with respect to the ones imposed as design requirements. This result is justified considering the lower than desired number of turns achieved during the prototype manufacturing and the inaccurate analytical modelling used to describe the valve magnetic circuit. A revision of the magnetic model towards the development of an HFMEC (High Fidelity Magnetic Equivalent Circuit) [15] is currently under development.

Further tests are foreseen in order both to more deeply investigate the performances of the designed actuators and to validate some undergoing modelling using bond-graph approach. In particular, this last point is useful to underline and characterize the relation between the module response with an imposed electrical power and a given loading power and comprehensively assess the reliability of the employed solution.

## References

- [1] Vékás L., *Ferrofluids and Magnetorheological Fluids*. Advanced in Science and Technology 54: 127-136 (2008).
- [2] Phulé P.P., *Magnetorheological (MR) Fluids: principles and applications*. Smart Materials Bulletin 2: 7-10 (2001).
- [3] Barnes H.A., Hutton J.F., Walters F.R.S., *An Introduction to Rheology*. Elsevier Science Publisher, Third Impression (1993).
- [4] Olabi A.G., Grunwald A., *Design and Application of magneto-rheological fluid*. Materials and Design 28: 2658-2664 (2007).
- [5] Carlson J.D., *MR Fluids and Devices in the Real World*. International Journal of Modern Physics B 7: 1463-1470 (2005).
- [6] Jolly M.R., Blender J.W., Carlson J.D., *Properties and Applications of Commercial Magnetorheological Fluids*. Journal of Intelligent Materials and Structures 10(1): 5-13 (1999).
- [7] Yavuz M., Erdemir A., Botek G. et al., *Peak Plantar Pressure and Shear Location*. Diabetes Case 30(10): 2643-2645 (2007).
- [8] Perry J.E., Hall J.O., Davis B.L., *Simultaneous measurement of plantar pressure and shear forces in diabetic individuals*. Gait and Posture, pp. 101-107 (2002).
- [9] Grivon D., Civet Y., Pataky Z., Perriard Y., *Design and Characterization of a Soft Miniature Magneto-Rheological Shock Absorber*. 10<sup>th</sup> International Symposium on Linear Drives for Industry Applications, July 27-29, Aachen, Germany (2015).
- [10] Grivon D., Civet Y., Pataky Z., Perriard Y., *Design and comparison of different Magneto-Rheological valve configurations*. IEEE/ASME International Conference on Advanced and Intelligent Mechatronics, 7-11 July, Busan, Korea (2015).
- [11] Phillips R.W., *Engineering applications of fluid with variable yield stress*. PhD Thesis, University of California Berkeley (1969).
- [12] Dai G., Biron Bird R., *Radial flow of Bingham fluid between two fixed circular disks*. Journal of Non-Newtonian Fluid Mechanics 8: 349-355 (1981).
- [13] Lord Corporation, Available online at <http://www.lord.com/> accessed July 2015.
- [14] AK Steel International, ARMCO Pure Iron, Available online at <http://www.aksteel.com/>, accessed July 2015.
- [15] Bartdoff M.A., Lumkes J.H., *High-Fidelity Magnetic Equivalent Circuit Model for an Axisymmetric Electromagnetic Actuator*. IEEE Transactions on Magnetics 45(8): (2009).